

“ MULTIDISCIPLINARY STUDIES OF DIFFUSE SOIL CO₂ FLUX, GAS PERMEABILITY, SELF-POTENTIAL, SOIL TEMPERATURE HIGHLIGHT THE STRUCTURAL ARCHITECTURE OF FONDI DI BAIJA CRATERS (CAMPI FLEGREI CALDERA, ITALY) ”

Luca Tarchini^{*,1,2}, Massimo Ranaldi², Maria Luisa Carapezza¹, Maria Giulia Di Giuseppe³, Roberto Isaia³, Carlo Lucchetti⁴, Ernesto Paolo Prinzi⁵, Francesco D’Assisi Tramparulo³, Antonio Troiano³, Stefano Vitale^{3,5}

⁽¹⁾ Dipartimento di Scienze, Università Roma TRE, Rome, Italy

⁽²⁾ Istituto Nazionale di Geofisica e Vulcanologia, Sezione di Roma 1, Rome, Italy

⁽³⁾ Istituto nazionale di Geofisica e Vulcanologia, Sezione di Napoli Osservatorio Vesuviano, Napoli, Italy

⁽⁴⁾ Dipartimento di Scienze della Terra, Università di Roma “La Sapienza”, Rome, Italy

⁽⁵⁾ Dipartimento Scienze della Terra, dell’Ambiente e delle Risorse (DiSTAR), Università di Napoli, Napoli, Italy

Article history

Received March 15, 2018; accepted August 28, 2018.

Subject classification:

Geochemical exploration; Magnetic and electrical methods; Structural geology; Gases; Volcanic risk.

ABSTRACT

We present in this paper the results of a geophysical and geochemical survey of self potential, diffuse soil CO₂ flux, soil temperature and gas permeability carried out in the Fondi di Baia craters on the western sector of Campi Flegrei caldera, one of the most hazardous active volcano in Italy. Work was aimed at highlighting the small-scale volcano-tectonic structures of this Holocene edifice and at evaluating its state of fracturing, in order to ascertain possible volcanic hazard for future vent reopening. The central sector of Campi Flegrei (Solfatara volcano-Pisciarelli) is indeed the one most affected by ground deformation and intense high-temperature fumarolic activity, nevertheless it cannot be ruled out a future vent opening along the western collapsed margin of the caldera, where Fondi di Baia craters are located. Our results show that the Fondi di Baia craters are characterized by a medium-high release of hydrothermal fluids through fractures that mimic the main volcano-tectonic structures of this portion of the caldera. Moreover, results indicate that, in case of a future volcanic re-activation, these previous structures could as well be possible paths for magma ascent. We provide a first estimate of the total flux of CO₂ from Fondi di Baia diffuse degassing structure, quantified in $10.06 \pm 1.07 \text{ t}^*\text{d}^{-1}$.

1. INTRODUCTION

Campi Flegrei caldera and Vesuvius volcano are the southernmost active portion of the Quaternary volcanic belt, aligned with the NW-SE trending Tyrrhenian extensional margin of central and southern Italy [e.g. Serri et al., 1993]. Campi Flegrei caldera is one of the most hazardous volcano in the world, due to its young age and the ubiquitous presence of several monogenic and polygenic volcanic centers. Presently the majority of researches and monitoring is fo-

cused on the central sector of the caldera where ground deformation and degassing are prevailing, such as in the Solfatara volcano and Pisciarelli area [e.g. Isaia et al., 2015; Chiodini et al., 2016]. However, recent studies [Selva et al., 2012; Bevilacqua et al., 2015, 2017] indicate a moderate probability for new vents opening also in the western sector of the Campi Flegrei. Hence, we present a geophysical and geochemical study of the Fondi di Baia craters (Figure 1). This multidisciplinary study of self potential, soil CO₂ flux, soil temperature and gas permeability of soils, is

aimed to identify buried volcano-tectonic structures and to evaluate their present state of activity. Simultaneous measurements have been performed, because of their relevance to hydrothermal activity [Finizola et al., 2003]. Emission of CO₂ from soil to atmosphere can be generated by different processes both biological (the so called “soil respiration”) and endogenous like the release from magma bodies or hydrothermal reservoirs. Surveys of diffuse CO₂ flux or in-soil gas concentration succeeded in finding anomalies in zones often corresponding to faults [Aubert and Baubron, 1988; D’Alessandro et al., 1992; Barberi and Carapezza, 1994; Giannamano et al., 1997, 1998; Allard et al., 1998; Azzaro et al., 1998; Etiopie et al., 1999]. CO₂ anomalies on active volcanoes are generally associated with highly permeable zones, which may also drain heat and other fluids [e.g. Finizola et al., 2003; Aubert and Baubron, 1988]. Hydrothermal systems in volcanic environments usually generate high amplitude SP anomalies [Zablocki, 1976; Aubert et al., 1984; Aubert and Dana, 1994; Di Maio and Patella, 1994; Malengreau et al., 1994; Zlotnicki et al., 1994; Patella, 1997; Finizola et al., 1998; Lénat et al., 1998], mainly due to streaming potential [Corwin and Hoover, 1979] related to

shallow water flow in the hydrothermal system. Several authors presented analysis and integration of geochemical, temperature and electrical data [e.g. Finizola et al., 2003; Lewicki et al., 2003; Revil et al., 2011], a few of them specifically devoted to the Campi Flegrei area [Bruno et al., 2007; Gresse et al., 2017; Di Giuseppe et al., 2017].

Self potential, soil CO₂ flux, soil temperature and soil gas permeability are parameters correlated to volcano-stimulated hydrothermal activity. Concurrent measures presented in this work, the analysis of their anomaly patterns, coupled with the examination of the geologic observations, led us to a funded structural interpretation, which outlines the circulation of hydrothermal fluids below the Fondi di Baia craters through volcano-tectonic structures and points to a possible hazard in case of a future vent reopening.

2. GEOLOGICAL SETTING

The Campi Flegrei area includes a ~12 km wide caldera (Figure 1), consisting of two nested down-sag collapses [Barberi et al., 1991; Acocella, 2008].

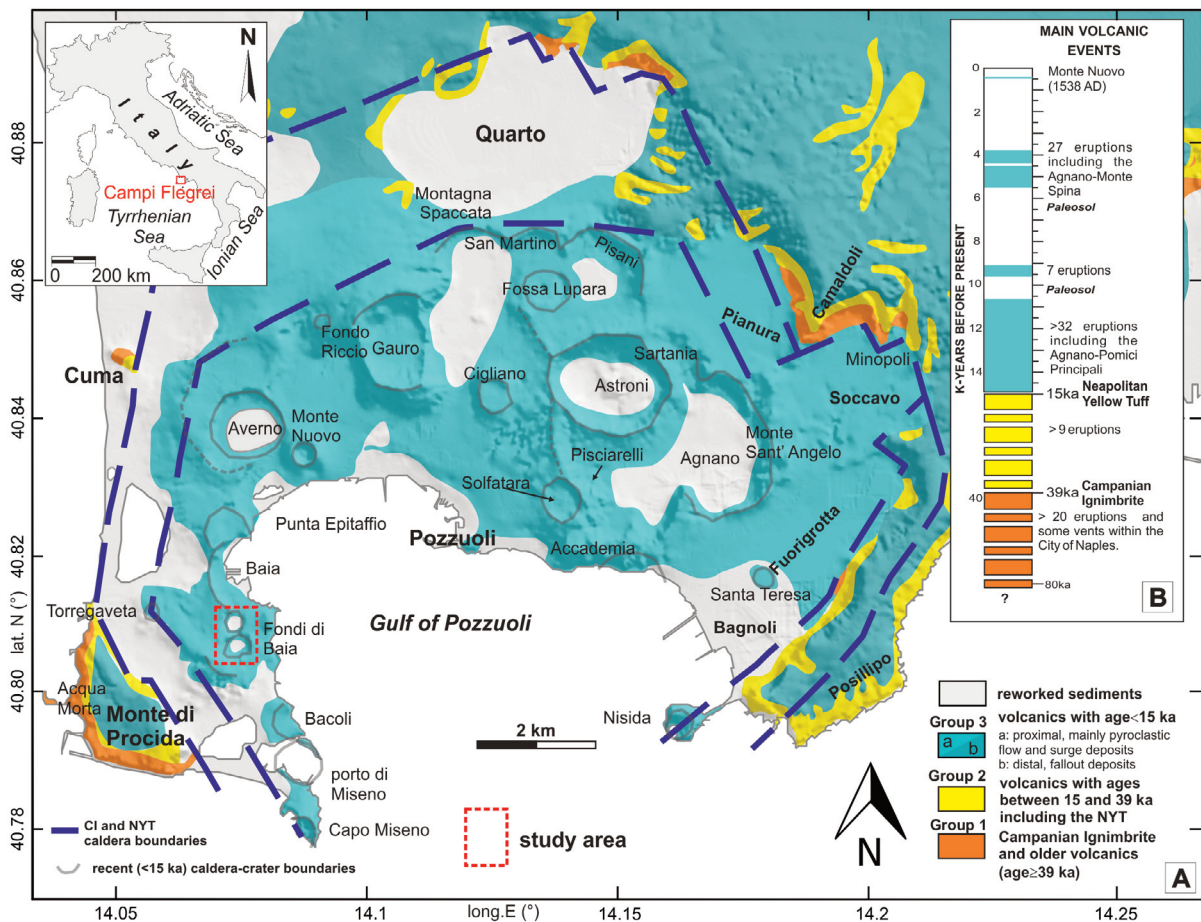


FIGURE 1. (A): Structural-geological map of Campi Flegrei (modified from Vitale and Isaia, 2014) showing location of the study area and of the main degassing sites of Solfatarà and Pisciarelli. (B) Main volcanic events in the CF.

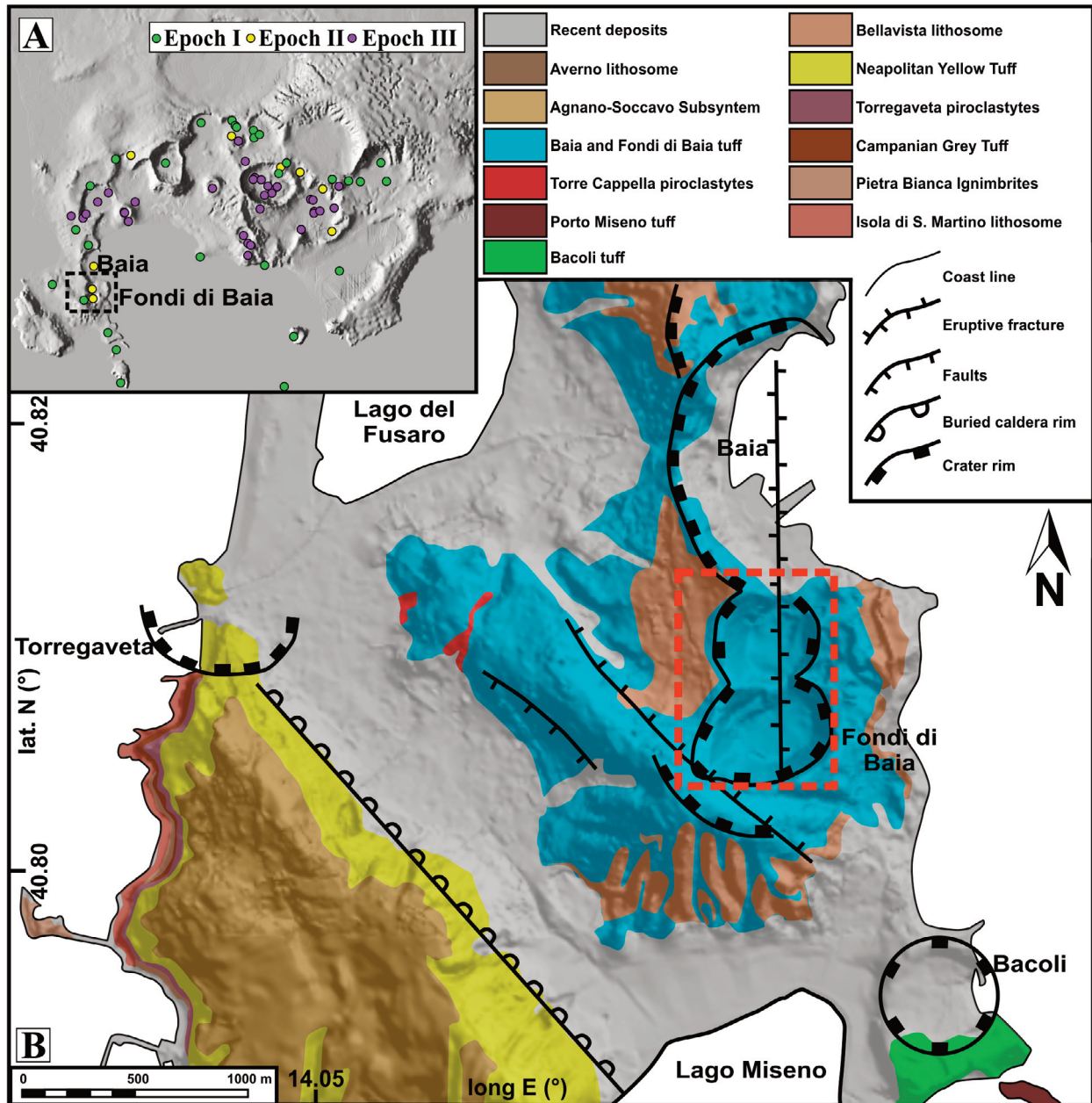


FIGURE 2. A) Location of eruptive vents younger than the TGN eruption (green circle= Epoch I; yellow circle= Epoch II; purple circle= Epoch III) [after D'Antonio et al., 1999]. Black dashed rectangle shows location of: B) Geologic map of Baia-Procida-Miseno sector (from Carta Geologica d'Italia 1:50000, Sheet Nr. 447 - NAPOLI; http://www.isprambiente.gov.it/Media/carg/447_NAPOLI/Foglio.html). Red dashed rectangle locates the investigated Fondi di Baia craters.

Two major eruptions of Campi Flegrei, the strongest in the Mediterranean area, were responsible for the outer and inner collapses (Figure 1): respectively the ~40 ka Campanian Grey Tuff –TGC– or Campanian Ignimbrite [Barberi et al., 1978; Rosi et al., 1983; Rosi and Sbrana, 1987] and the ~15 ka Neapolitan Yellow Tuff –TGN– [Orsi et al., 1992; Scarpato et al., 1993; Wohletz et al., 1995].

After each caldera collapse, volcanism restricted along the borders and within the collapsed portion, thus all the <15 ka eruptive vents aligned along the TGN caldera or opened especially in its northeastern sector (Figure 2A)

[D'Antonio et al., 1999; Di Vito et al., 1999; Wohletz et al., 1999; Bevilacqua et al., 2015]. At least 70 eruptive events occurred until recent times, prevalently phreatomagmatic with low to medium magnitude (volumes <0.1 km³) [Di Renzo et al., 2011]. These eruptions have been grouped into three eruptive epochs separated by periods of quiescence marked by two paleosoils: Epoch1 spanning 15 to 10.6 ka BP; Epoch2 (9.6 to 9.1 ka BP); and Epoch3 (5.5 to 3.5 kya BP) [Di Vito et al., 1999; Isaia et al., 2009; Smith et al., 2011]. The most recent event was the Monte Nuovo eruption of 1538 BCE [Guidoboni

and Ciuccarelli, 2011; Di Vito et al., 2016].

Baia–Fondi di Baia eruptions (Figure 2), dated at 9.696–9.525 ka [Smith et al., 2011], opened the second epoch after a 1000 year-long quiescence. Pistolesi et al. [2017] reported a complete study of stratigraphy and chemistry of these events, to which we refer for detailed description and discussion on eruptive dynamics. Authors recognize five units, belonging to two eruptive phases separated by short time break. The Baia episode developed in a shallow water environment and produced a basal breccia followed by alternation of purely magmatic fall-out and pyroclastic density current (PDC) deposits. Vents shifted southwards and on-land during this phase. Fondi di Baia phase took place at the southernmost sector (Figure 2) after a short time lapse, with the emplacement of an opening breccia unit followed by PDCs and obsidian ballistic deposits [Pistolesi et al., 2017].

3. METHODS

Diffuse soil CO₂ flux measurements were performed with the accumulation chamber methodology [Chiodini et al., 1998] by placing an open-bottomed chamber directly on the soil surface. The contained air, enriched in effusing soil CO₂, was circulated within the chamber by a fan and its CO₂ concentration ([CO₂]) was measured every second by means of a Li-COR820 non-dispersive infrared gas analyzer (accuracy < 3% of reading). Soil CO₂ diffuse flux was calculated from the [CO₂] vs. time gradient.

Soil temperature was measured at 0.2 m depth with a DeltaOhm HD2301.0 portable thermometer with a PT473P penetration probe (Accuracy ±0.25 °C) on the same points of soil CO₂ flux.

Gas permeability of soils was measured at 0.8 m depth with the PRM3 permeameter manufactured at the Geochemistry Lab of Roma TRE University. Theoretical framework of the PRM3 permeameter is based on Darcy's equation, where the soil is assumed to be homogeneous and isotropic and standard conditions are considered. A constant cavity was created at the bottom of a probe driven into the soil at 0.8 m depth. Air was pumped out from the soil by a miniature vacuum pump. The intrinsic gas permeability was then calculated by measuring the pressure difference between atmosphere and probe, as described in Castelluccio et al. [2015].

Self-potential survey was conducted by mapping the quasi-static natural electrical field at the ground surface,

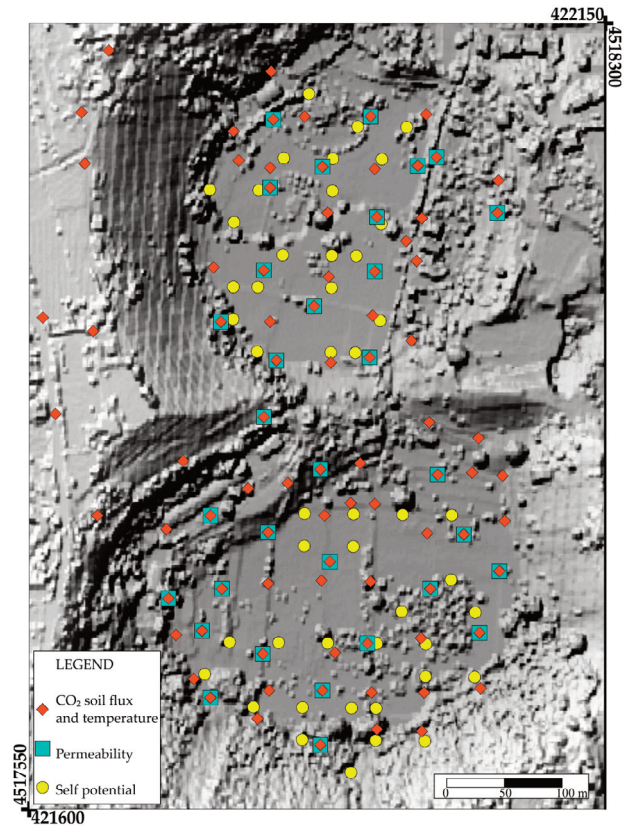


FIGURE 3. Location of the CO₂ flux and temperature (red diamond), gas permeability (light blue square) and self potential (yellow circle) measurements. Vertex coordinates are in UTM, projection WGS84 33N.

following the rationale presented in Di Maio et al. [1996]. The measurement equipment consisted of a high-impedance voltmeter, a pair of Cu/CuSO₄ non-polarizing electrodes and an insulated electric cable.

Potential drops were acquired across a passive dipole (50 m in length) continuously displaced along interconnected circuits linking the points reported in Figure 3. An optimal electrical contact with the ground was retrieved (always <200 kΩ and generally <20 kΩ). The SP drops were detected one after the other between every two consecutive position of the electrodes (leapfrog technique), after reaching stable signal conditions. The adopted acquisition method involved averaging a set of data sampled at a constant time interval over a period of tens of seconds. In order to eliminate drift and/or locally spurious signals, the close circuits were surveyed by turning back to the initial point and the misfit was equally distributed over all dipolar SP drops.

Approximately 0.25 km² of the Fondi di Baia craters were surveyed by mean of 85 measurements of soil CO₂ flux and temperature; 0.10 km² by 48 self potential measurements; and 0.18 km² by 32 gas permeability mea-

surements (Figure 3). Measurements were made at the crater bottom, and over the slopes when possible, depending on morphology and free access to private areas, thus sampling scheme resulted in a random, but not clustered, pattern throughout the surveyed area.

4. RESULTS

Diffuse soil CO₂ flux ranged from 14.8 to 96.2 g*m⁻²d⁻¹, with a mean of 30.7 g*m⁻²day⁻¹. Soil temperature spanned 9.4 to 19.2 °C, with a mean of 14.6 °C. Gas permeability ranged from 3.9*10⁻¹³ to 8.0*10⁻¹¹ m², with a mean of 2.1*10⁻¹¹ m². Self potential varied from -75.0 to 47.0 mV (average = -19.6 mV) (Table 1).

			Proportion %	Min	Max	Avg	Std Dev
Gas Permeability	k (m ²)	Population A	67.12	3.86*10 ⁻¹³	2.67*10 ⁻¹¹	1.14*10 ⁻¹¹	8.10*10 ⁻¹²
		Population B	32.88	3.99*10 ⁻¹¹	7.95*10 ⁻¹¹	4.00*10 ⁻¹¹	2.21*10 ⁻¹¹
Self Potential	SP (mV)		100.00	-75.0	47.0	-19.6	23.5
Soil CO ₂ flux	Φ(g m ⁻² d ⁻¹)	Population A	40.96	14.8	23.2	19.0	2.6
		Population B	42.08	23.5	40.5	30.2	6.1
		Population C	16.96	43.9	96.2	60.6	18.3
Temperature	T (°C)		100.00	9.4	19.2	14.6	2.5

TABLE 1. Main statistical parameters of the Fondi di Baia measurements.

Figure 4 shows the normal probability plots of the field measurements. Although CO₂ flux, gas permeability and self potential data seem to be skewed, indeed a log-likelihood criterion shows that only self potential and temperature are normally distributed. Conversely, gas permeability and CO₂ flux data are respectively bimodal and trimodal. Statistical analyses and distribution assessment were made in Matlab® R2017a.

Based on the normal probability plot of gas permeability (light blue squares in Figure 4), we can evidence a change in slope at k=3.33*10⁻¹¹ m² (33.3 pm²). This value separates data characterized by low-medium gas permeability from high k measurements (Table 1). Similarly, in the normal probability plot of CO₂ flux (red diamonds in Figure 4) we can evidence two changes in slope, one at 23.3 and another at 42.2 g*m⁻²d⁻¹. Table 1 reports the main statistics of the field measurements.

Emission of CO₂ from soil to atmosphere can be generated by different processes both biological (the so called “soil respiration”) and endogenous like the release from magma bodies or hydrothermal reservoirs. Generally soil

respiration CO₂ fluxes are lower than few tens of g*m⁻²d⁻¹ [e.g. Rey et al., 2002; Carapezza et al., 2015], while hydrothermal or magmatic diffuse effluxes span tens to several thousands of g*m⁻²d⁻¹, like in the near Solfatara di Pozzuoli degassing area [Chiodini et al., 2010]. Thus, we considered fluxes up to 23.3 g*m⁻²d⁻¹ belonging to soil respiration processes. Conversely, CO₂ fluxes higher than 42.2 g*m⁻²d⁻¹ are fed by a weak hydrothermal anomaly. Intermediate fluxes are likely to be considered as a mixing between the two sources (Table 1).

The maps of permeability, self potential, soil CO₂ flux and temperature (Figure 5) were made with ordinary kriging in Golden Software, Inc. Surfer11®. Each interpolated grid has the same geometry, being composed by 6x6 m cells. Furthermore, grid cells of soil CO₂ flux, soil tem-

perature, gas permeability and self potential are all fully stacked. However, each grid has been extrapolated only within the area covered by the relative field measurements (Figure 5). Each map has a customized color scale in order to highlight sectors characterized by different geophysical or geochemical patterns.

In the soil CO₂ flux map (Figure 5A), blue colors show zones with soil respiration fluxes. Green colors indicate areas of intermediate flux. Yellow to orange colors highlight zones characterized by high CO₂ release. High soil flux values are roughly NNW-SSE aligned in the western sector out of the crater rim, and NNE-SSW aligned in the central investigated area at the craters bottom. The total CO₂ emission rate from the investigated area could also be calculated, given the kriging estimates and the partitioning of CO₂ measures into three flux classes. The CO₂ flux from soil respiration is calculated in 1.05 ± 0.10 t*d⁻¹ from 45,144 m². The CO₂ emissions from the intermediate flux class are calculated in 7.25 ± 0.78 t*d⁻¹ from 171,972 m². Finally, CO₂ emission rate for the hydrothermal source sums up to 2.81 ± 0.29 t*d⁻¹ from an

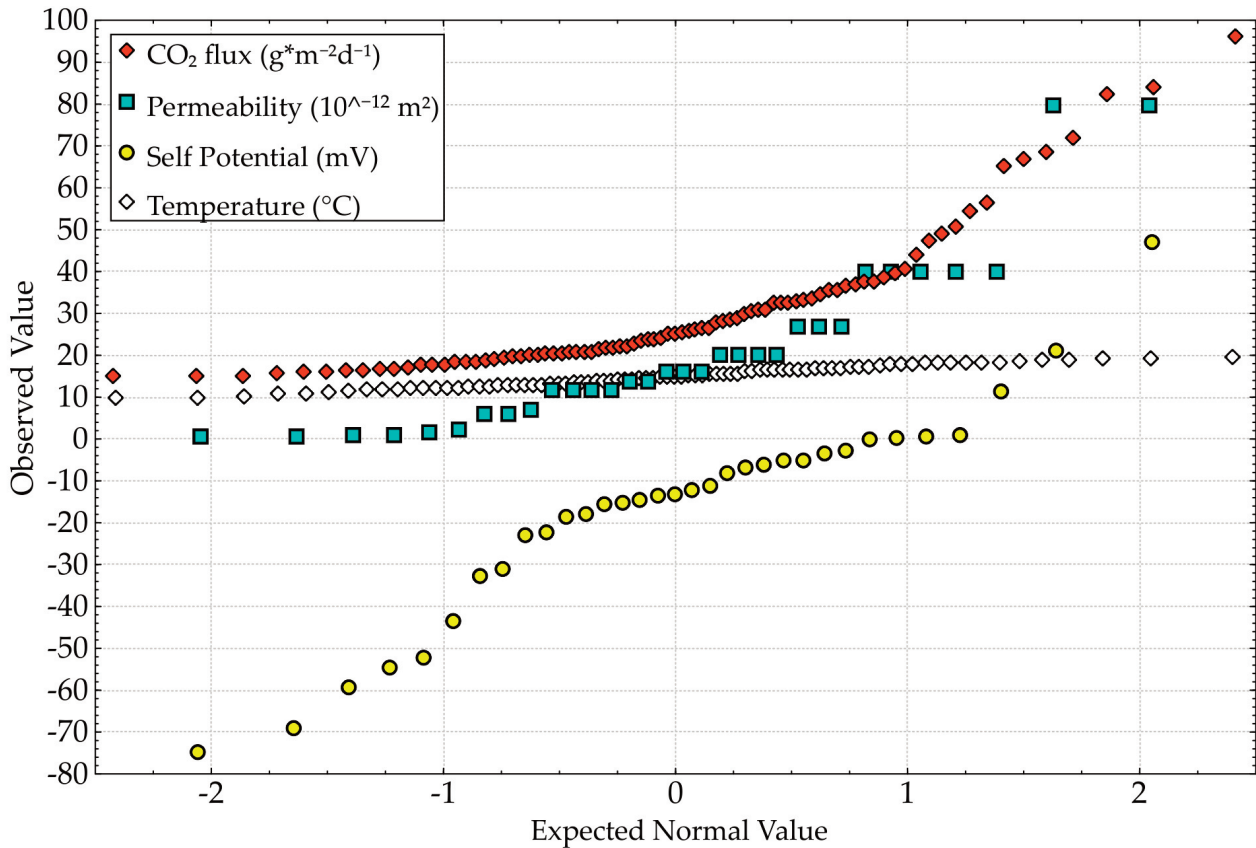


FIGURE 4. Normal probability plot of Fondi di Baia measurements. Gas permeability is expressed in pm^2 .

area of $29,412 \text{ m}^2$.

Considering the sum of the two latter contributions, Fondi di Baia crater area releases $10.06 \pm 1.07 \text{ t} \cdot \text{d}^{-1}$ from an anomalous area of $\sim 200,000 \text{ m}^2$.

The gas permeability map (Figure 5B) evidence zones of very low gas permeability with blue colors, medium permeability in light yellow colors, and high gas permeability in orange colors. Gas permeabilities are lowest in each of the two crater bottoms, while maxima align in a NNW-SSE direction, which partly superimposes to the central CO_2 anomaly.

In Figure 5C, blue colored zones are characterized by low soil temperature (below $15.1 \text{ }^\circ\text{C}$; corresponding to the 95% Student's-t upper confidence limit of a normal distribution) and two yellow areas fence soil temperatures above $17.5 \text{ }^\circ\text{C}$. Soil temperatures are ubiquitously low in the northern crater, but two higher T areas are found in the southern portions. A first area, NNW-SSE elongated, matches the CO_2 maxima outside the western crater rims. Another high T area is present at the southern crater bottom and has a semicircular shape that partly stacks over both soil flux and gas permeability maxima.

Areas with self potential (SP) lower than -20 mV are blue-colored; areas with SP spanning -20 to 0 mV are

light blue-colored; Orange colors evidence sectors with positive SP (Figure 5D). An area of SP down to -75 mV is only found in the northern crater, while the southern one is characterized by mild negative SP values (min $\sim -50 \text{ mV}$) in the middle and at the southernmost corner. Positive areas occur along the slope-feet to the north, the south and in the center of the investigated area.

5. DISCUSSIONS

Geochemical and geophysical results indicate a low volcano activity mainly related to the hydrothermal degassing, furthermore the maps of self potential, temperature, gas permeability and soil CO_2 flux (Figure 5) evidence zones with contrasting geophysical and geochemical behaviors that in turn highlight possible volcano-tectonic structures.

The highest measured CO_2 fluxes are not comparable to those measured at the Solfatara crater and Pisciarelli area, which can be orders of magnitude higher [Chiodini et al., 2010]. Nevertheless, soil CO_2 flux values measured at Fondi di Baia are higher than typical soil respiration fluxes of central Italy [Rey et al., 2002; Carapezza et al.,

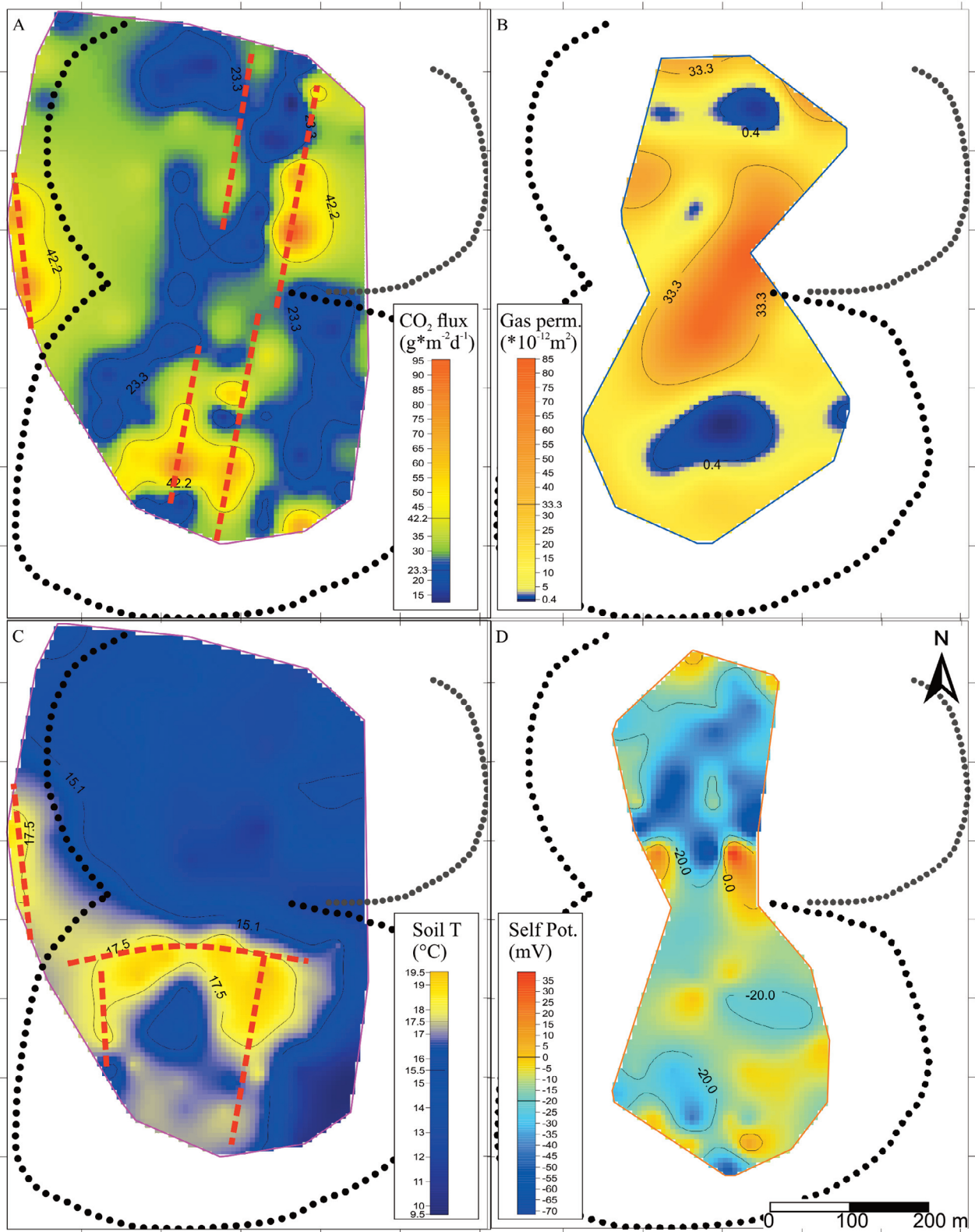


FIGURE 5. Maps of A) Soil CO₂ flux; B) Gas permeability (in 10^{-12} m^2); C) Soil temperature; D) Self potential. Dotted line= crater rims. Red dashed line= inferred lineaments, as described in text. Purple line= perimeter of CO₂ flux and soil temperature measurements. Blue line= perimeter of gas permeability measurements. Orange line= perimeter of self potential measurements. Each map has the same vertex coordinates of Figure 3.

2015]. Values above 40 and up to ca. $100 \text{ g}\cdot\text{m}^{-2}\cdot\text{d}^{-1}$ are likely low fluxes from a hydrothermal source contaminated by air entering from highly fractured and perme-

able terrains. Similar findings were made on other volcanic-hydrothermal areas of Italy: e.g. Vesuvio cone [Froncini et al., 2004; Granieri et al., 2013], Stromboli

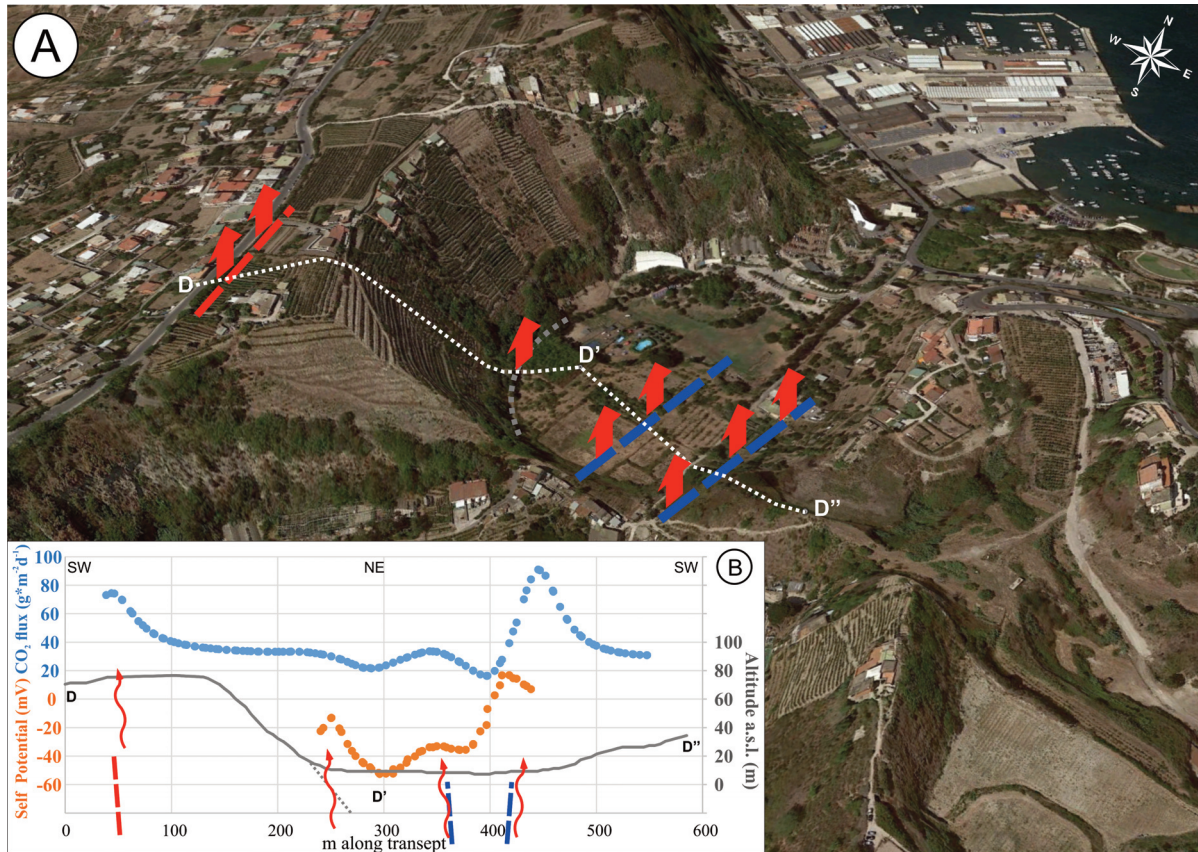


FIGURE 6. A) Main inferred buried fractures (dashed blue and grey lines) and faults (dashed red line) of Fondi di Baia craters, inferred from self potential and soil flux data along a transverse transect (white stippled line) through the northern crater. B) Self potential (orange dots) and CO₂ soil flux (blue dots) values along the transect. The full grey line shows the elevation along the trace section. Red arrows indicate the main inferred hydrothermal pathways.

[Carapezza et al., 2009] or Colli Albani [Carapezza et al., 2012].

Maps of soil CO₂ fluxes (Figure 5A) evidence two main mild degassing lineaments clearly aligned along two directions (respectively NNE-SSW and NNW-SSE) at the crater bottoms and outside the western rim. NNE-SSW directed degassing zone is consistent with the alignment of the centers of Fondi di Baia craters and Baia crater, the latter currently partially exposed (Figure 1). We suggest that this lineament can correspond to the feeding fracture of these three volcanoes. Furthermore, this degassing zone is about parallel to the main fault reported in the official cartography (Figure 2). Total CO₂ efflux from abiogenic source is evaluated at $10.06 \pm 1.07 \text{ t}\cdot\text{d}^{-1}$, which means that Fondi di Baia is a medium-high intensity degassing structure.

A NNE-SSW/NE-SW alignment is also depicted by high gas permeability ($> 3.33 \cdot 10^{-11} \text{ m}^2$) across the two craters (Figure 5B). This alignment clearly corresponds to the high CO₂ flux one. Gas permeability of soils is instead very low ($< 4.0 \cdot 10^{-13} \text{ m}^2$) to the north and to the south of this lineament. Such features indicate the

presence of self-sealing phenomena, alike observable at the bottom of other craters [e.g. La Fossa di Vulcano; Granieri et al., 2006, 2014].

The temperature map of Figure 5C shows a warmer area to the west that corresponds to the high CO₂ flux sector outside the crater rims. Another warmer area, with a semi-annular shape, occurs at the bottom of the southern crater and it almost encircles the low gas permeability zone. Measured temperatures (Table 1) are not high compared to soil temperatures of other volcanic centers which can be as high as the water boiling temperature when standing on a bi-phase hydrothermal system, or even higher [Chiodini et al., 2005]. Nevertheless, soil temperature was measured in late autumn, so a heating by solar radiation can be ruled out. Likely, such temperature anomalies point to a weak release of hydrothermal fluids, but only beneath the southern crater. We envisage the occurrence of a main E-W fault that separates the two craters and other two structures NNW-SSE and NNE-SSW directed located in the bottom of the southern crater (Figure 5C).

Also self potential characteristics are different be-

tween the two Fondi di Baia craters (Figure 5D). The northern one has, in fact, lower values (down to -75 mV) with respect to the southern one. Likely, the negative SP anomalies are due to a streaming potential from circulation of meteoric water. In addition, the mildly negative SP anomalies of the southern crater are a combination of streaming potential and of a positive signal due to upflow of hydrothermal fluids.

Finally, in Figure 6, we show the inferred faults/fissures, resulting from the geophysical and geochemical maps analysis. In order to evidence the links between local tectonics and surveyed data, we extrapolated a transect of both self potential and soil flux from the relative maps.

This SW-NE/NE-SW transect (white stippled line in Figure 6A) cuts through the main anomalies of the northern crater that is displayed in a Google Earth 3D bird's eye view. Figure 6B shows the variation of self potential (orange dots) and soil flux (blue dots) along the trace. Three clear anomalies are found: i) the western one (red dashed line) is likely related to a buried fault whose orientation connects to the caldera collapse; ii) at the crater center two parallel anomalies (blue dashed line) are linked to the main feeding fissure; iii) the last one (grey dashed line) stands along the crater bottom and is likely connected to the border fracturing produced by the vent opening.

Such as discussed before, the buried structure of the Fondi di Baia craters is hence characterized by a NNE-SSW oriented structure likely corresponding to the main feeder fissure, and other additional structures such as a NNW-SSE caldera fault and large fractured zones along the vents borders.

6. CONCLUSIONS

We investigated Fondi di Baia craters by a multidisciplinary survey of self potential, gas permeability, soil CO₂ flux and temperature. This study adds new information for the reconstruction of buried volcano-tectonic structures in this sector, highlighted by a mild circulation of hydrothermal fluid. In fact, diffuse soil CO₂ flux, soil temperatures, self potential and gas permeability clearly trace volcano-tectonic structures. One of these structures is a small caldera fault that lies westward of the crater rims. Other features, occurring within both craters with a NNE-SSW direction, are likely connected to the highly fractured zone of the primary feeding fissure.

In addition, all the geophysical and geochemical data evidence a midsize, but clear, circulation of hydrothermal fluids especially below the southern crater. Gas permeability is lowest at the crater centers for self-sealing processes. Soil temperature anomalies have a semi-annular shape surrounding the low gas permeability area. The mid-negative self potential values are likely due to overlapping of streaming potential of shallow groundwater with ascending hydrothermal fluids. Soil CO₂ flux follows the temperature pattern at the crater bottom and pursues towards NNE along the feeding fracture. The total release from a hydrothermal source is calculated in 10.06 ± 1.07 tons of CO₂ per day from a $\sim 200,000$ m² area.

Findings, compared to available and original structural and stratigraphic data, well integrate in the general volcanic scenario of the Campi Flegrei. Concurrent geochemical and geophysical investigations highlighted previous structures that mimic the local volcano-tectonic pattern. Our results thus indicate that the borders of the resurgent caldera are possible sites of future vent opening, as well as is, obviously, the most strained central portion [Selva et al., 2012; Bevilacqua et al., 2015, 2017].

Acknowledgements. We acknowledge Enrico Cascella, Erik Conti, Nicola Castello, Alessandro Cicatiello, Marco Maiolino, Domenico Puzio, Lucia Tazza and Roberto Villani for their help in the field surveys. We thank the anonymous reviewers for their suggestions and comments, which improved the paper.

REFERENCES

- Acocella, V. (2008). Activating and reactivating pairs of nested collapses during caldera-forming eruptions: Campi Flegrei (Italy). *Geophys. Res. Lett.*, 35(17).
- Allard, P., G. Hammouya and F. Parello (1998). Diffuse magmatic soil degassing at Soufrière of Guadeloupe, Antilles. *C. R. Acad. Sci. Paris*, 327, 315–318.
- Aubert, M., R. Auby, F. Bourley and Y. Bourley (1984). Contribution à la surveillance de l'activité de l'Etna à partir de l'étude des zones fumeroliennes. *Bull. Volcanol.*, 47, 1039–1050.
- Aubert, M. and J.C. Baubron (1988). Identification of a hidden thermal fissure in a volcanic terrain using a combination of hydrothermal convection indicators and soil-atmosphere analysis. *J. Volcanol. Geotherm. Res.*, 35, 217–225.

- Aubert, M. and I. Dana (1994). Interprétation des profils radiaux de polarisation spontanée (PS) en volcanologie. Possibilités d'application de la méthode PS à la surveillance des volcans actifs. *Bull. Soc. Géol. France*, 165, 113–122.
- Azzaro, R., S. Branca, S. Giammanco, S. Gurrieri, R. Rasà and M. Valenza (1998). New evidence for the form and extent of the Pernicana Fault System (Mt Etna) from structural and soil-gas surveying. *J. Volcanol. Geotherm. Res.*, 84, 143–152.
- Barberi F. and M.L. Carapezza (1994). Helium and CO₂ soil gas emission from Santorini (Greece). *Bull. Volcanol.*, 56, 335–342.
- Barberi, F., E. Cassano, P. La Torre and A. Sbrana, (1991). Structural evolution of Campi Flegrei caldera in light of volcanological and geophysical data. *J. Volcanol. Geotherm. Res.*, 48(1–2), 33–49.
- Barberi, F., F. Innocenti, L. Lirer, R. Munno, T. Pescatore and R. Santacroce (1978). The Campanian Ignimbrite: a major prehistoric eruption in the Neapolitan area (Italy). *Bull. Volcanol.*, 41(1), 10–31.
- Bevilacqua, A., F. Flandoli, A. Neri, R. Isaia and S. Vitale (2016). Temporal models for the episodic volcanism of Campi Flegrei caldera (Italy) with uncertainty quantification. *J. Geophys. Res.: Solid Earth*, 121(11), 7821–7845.
- Bevilacqua, A., R. Isaia, A. Neri, S. Vitale, W.P. Aspinall, M. Bisson, F. Flandoli, P.J. Baxter, A. Bertagnini, T. Esposti Ongaro, E. Iannuzzi, M. Pistolesi and M. Rosi (2015). Quantifying volcanic hazard at Campi Flegrei caldera (Italy) with uncertainty assessment: 1. Vent opening maps. *J. Geophys. Res.: Solid Earth*, 120(4), 2309–2329.
- Bruno, P.P.G., G.P. Ricciardi, Z. Petrillo, V. Di Fiore, A. Troiano and G. Chiodini (2007). Geophysical and hydrogeological experiments from a shallow hydrothermal system at Solfatara Volcano, Campi Flegrei, Italy: Response to caldera unrest. *J. Geophys. Res.: Solid Earth*, 112 (B6).
- Carapezza, M.L., F. Barberi, M. Ranaldi, T. Ricci, L. Tarchini, J. Barrancos, C. Fischer, C. Lucchetti, G. Melian, N. Perez, P. Tuccimei, A. Vogel and K. Weber (2012). Hazardous gas emissions from the flanks of the quiescent Colli Albani volcano (Rome, Italy). *Appl. Geochem.*, 27(9), 1767–1782.
- Carapezza, M.L., M. Ranaldi, A. Gattuso, N. Pagliuca and L. Tarchini (2015). The sealing capacity of the cap rock above the Torre Alfina geothermal reservoir (Central Italy) revealed by soil CO₂ flux investigations. *J. Volcanol. Geotherm. Res.*, 291, 25–34.
- Carapezza, M.L., T. Ricci, M. Ranaldi and L. Tarchini, (2009). Active degassing structures of Stromboli and variations in diffuse CO₂ output related to the volcanic activity. *J. Volcanol. Geotherm. Res.*, 182(3–4), 231–245.
- Castelluccio, M., G. De Simone, C. Lucchetti, M. Moroni, F. Salvati and P. Tuccimei (2015). A new technique to measure in situ soil gas permeability. *J. Geochem. Explor.*, 148, 56–59.
- Chiodini, G., S. Caliro, C. Cardellini, R. Avino, D. Granieri and A. Schmidt (2008). Carbon isotopic composition of soil CO₂ efflux, a powerful method to discriminate different sources feeding soil CO₂ degassing in volcanic-hydrothermal areas. *Earth Planet. Sci. Lett.*, 274(3–4), 372–379.
- Chiodini, G., S. Caliro, C. Cardellini, D. Granieri, R. Avino, A. Baldini, M. Donnini and C. Minopoli (2010). Long-term variations of the Campi Flegrei, Italy, volcanic system as revealed by the monitoring of hydrothermal activity. *J. Geophys. Res.*, 115, B03205.
- Chiodini, G., R. Cioni, M. Guidi, B. Raco and L. Marini (1998). Soil CO₂ flux measurements in volcanic and geothermal areas. *Appl. Geochem.*, 13(5), 543–552.
- Chiodini, G., D. Granieri, R. Avino, S. Caliro, A. Costa and C. Werner (2005). Carbon dioxide diffuse degassing and estimation of heat release from volcanic and hydrothermal systems. *J. Geophys. Res.: Solid Earth*, 110, B08204, doi: 10.1029/2004JB003542.
- Chiodini, G., J. Vandemeulebrouck, S. Caliro, L. D'Auria, P. De Martino, A. Mangiacapra and Z. Petrillo (2015). Evidence of thermal-driven processes triggering the 2005–2014 unrest at Campi Flegrei caldera. *Earth Planet. Sci. Lett.*, 414, 58–67.
- Corwin R.F. and D.B. Hoover (1979). The self-potential method in geothermal exploration. *Geophysics*, 44, 226–245.
- D'Alessandro, W., R. De Domenico, F. Parello and M. Valenza (1992). Soil degassing in tectonically active areas of Mt Etna. *Acta Vulcanol.*, 2, 175–183.
- D'Antonio, M., L. Civetta, G. Orsi, L. Pappalardo, M. Piochi, A. Carandente, S. de Vita, M.A. Di Vito and R. Isaia (1999). The present state of the magmatic system of the Campi Flegrei caldera based on a reconstruction of its behavior in the past 12 ka. *J. Volcanol. Geotherm. Res.*, 91(2), 247–268.
- Di Giuseppe, M.G., A. Troiano, M.A. Di Vito, R. Somma

- and F. Matano (2017). Definition of small-scale volcanic structures by Electrical Resistivity Tomography: the Trentaremi cone, an example from the Campi Flegrei Caldera (Italy). *Annals Geophys.*, 60(5), 0552.
- Di Maio, R. and D. Patella (1994). Self-potential anomaly generation in volcanic areas. The Mt Etna case-history. *Acta Vulcanol.*, 4, 119–124.
- Di Vito, M.A., V. Acocella, G. Aiello, D. Barra, M. Battaglia, A. Carandente, C. Del Gaudio, S. de Vita, G.P. Ricciardi, C. Ricco, R. Scandone and F. Terrasi (2016). Magma transfer at Campi Flegrei caldera (Italy) before the 1538 AD eruption. *Scientific reports*, 6, 32245, doi: 10.1038/srep32245.
- Di Vito, M.A., R. Isaia, G. Orsi, J.D. Southon, S. de Vita, M. D'Antonio, L. Pappalardo and M. Piochi (1999). Volcanism and deformation since 12,000 years at the Campi Flegrei caldera (Italy). *J. Volcanol. Geotherm. Res.*, 91(2-4), 221-246.
- Di Renzo, V., I. Arienzo, L. Civetta, M. D'Antonio, S. Tonarini, M.A. Di Vito and G. Orsi (2011). The magmatic feeding system of the Campi Flegrei caldera: architecture and temporal evolution. *Chem. Geol.*, 281(3), 227-241.
- Etiopie, G., P. Beneduce, M. Calcara, P. Favali, F. Frugoni, M. Schiattarella and G. Smriglio (1999). Structural pattern and CO₂-CH₄ degassing of Ustica Island, Southern Tyrrhenian basin. *J. Volcanol. Geotherm. Res.*, 88, 291–304.
- Finizola, A., D. Ramos and O. Macedo (1998). Self-potential studies of hydrothermal systems and structure on Misti and Ubinas volcanoes, South Peru. In: *Geophysicae A* (ed) 23rd EGS Meeting. Solid Earth Geophysics and Geodesy, Nice.
- Finizola, A., F. Sortino, J.F. Lénat, M. Aubert, M. Ripepe and M. Valenza (2003). The summit hydrothermal system of Stromboli. New insights from self-potential, temperature, CO₂ and fumarolic fluid measurements, with structural and monitoring implications. *Bull. Volcanol.*, 65(7), 486-504.
- Froncini, F., G. Chiodini, S. Caliro, C. Cardellini, D. Granieri and G. Ventura (2004). Diffuse CO₂ degassing at Vesuvio, Italy. *Bull. Volcanol.*, 66(7), 642-651.
- Giammanco, S., S. Gurrieri and M. Valenza (1997). Soil CO₂ degassing along tectonic structures of Mount Etna (Sicily): the Pernicana fault. *Appl. Geochem.*, 12, 429–436.
- Giammanco, S., S. Gurrieri and M. Valenza (1998). Anomalous soil CO₂ degassing in relation to faults and eruptive fissures on Mount Etna (Sicily, Italy). *Bull. Volcanol.*, 60, 252–259.
- Granieri, D., M.L. Carapezza, R. Avino, S. Caliro, C. Cardellini, G. Chiodini, M. Donnini, C. Minopoli, M. Ranaldi, T. Ricci and L. Tarchini (2013). Level of carbon dioxide diffuse degassing from the ground of Vesuvio: Comparison between extensive surveys and inferences on the gas source. *Ann. Geophys.*, 56(4), S0449.
- Granieri, D., M.L. Carapezza, F. Barberi, M. Ranaldi, T. Ricci and L. Tarchini (2014). Atmospheric dispersion of natural carbon dioxide emissions on Vulcano Island, Italy. *J. Geophys. Res.: Solid Earth*, 119(7), 5398-5413.
- Granieri, D., M.L. Carapezza, G. Chiodini, R. Avino, S. Caliro, M. Ranaldi, T. Ricci and L. Tarchini (2006). Correlated increase in CO₂ fumarolic content and diffuse emission from La Fossa crater (Vulcano, Italy): Evidence of volcanic unrest or increasing gas release from a stationary deep magma body? *Geophys. Res. Lett.*, 33(13).
- Gresse, M., J. Vandemeulebrouck, S. Byrdina, G. Chiodini, A. Revil, T.C. Johnson, T. Ricci, G. Vilardo, A. Mangiacapra, T. Lebourg, J. Grangeon, P. Bascou and L. Metral (2017). Three-Dimensional Electrical Resistivity Tomography of the Solfatara Crater (Italy): Implication for the Multiphase Flow Structure of the Shallow Hydrothermal System. *J. Geophys. Res.: Solid Earth*, 122(11), 8749–8768.
- Guidoboni, E. and C. Ciuccarelli (2011). The Campi Flegrei caldera: historical revision and new data on seismic crises, bradyseisms, the Monte Nuovo eruption and ensuing earthquakes (twelfth century 1582 AD). *Bull. Volcanol.*, 73(6), 655–677.
- Isaia, R., P. Marianelli and A. Sbrana (2009). Caldera unrest prior to intense volcanism in Campi Flegrei (Italy) at 4.0 ka BP: Implications for caldera dynamics and future eruptive scenarios. *Geophys. Res. Lett.*, 36(21).
- Isaia, R., S. Vitale, M.G. Di Giuseppe, E. Iannuzzi, F.D.A. Tramparulo, A. Troiano (2015). Stratigraphy, structure and volcano-tectonic evolution of Solfatara maar-diatreme (Campi Flegrei, Italy). *Geol. Soc. Am. Bull.*, 127, 1485–1504.
- Lénat, J.F., B. Robineau, S. Durand and P. Bachélery (1998). Etude de la zone sommitale du volcan Karthala (Grande Comore) par polarisation spontanée. *C. R. Acad. Sci.*, 327, 781–788.

- Lewicki, J.L., C. Connor, K. St-Amand, J. Stix and W. Spinner (2003). Self-potential, soil CO₂ flux, and temperature on Masaya volcano, Nicaragua. *Geophys. Res. Lett.*, 30(15), 1817.
- Malengreau, B., J.F. Lénat and A. Bonneville (1994). Cartographie et surveillance temporelle des anomalies de Polarisation Spontanée (PS) sur le Piton de la Fournaise. *Bull. Soc. Géol. Fr.*, 165, 221–232.
- Moretti, R., G. De Natale and C. Troise (2017). A geochemical and geophysical reappraisal to the significance of the recent unrest at Campi Flegrei caldera (Southern Italy). *Geochem. Geophys. Geosyst.*, 18(3), 1244–1269.
- Orsi, G., M. D'Antonio, S. de Vita and G. Gallo (1992). The Neapolitan Yellow Tuff, a large-magnitude trachytic phreatoplinian eruption: eruptive dynamics, magma withdrawal and caldera collapse. *J. Volcanol. Geotherm. Res.*, 53(1-4), 275–287.
- Patella, D. (1997). Self-potential global tomography including topographic effects. *Geophys. Prospect.*, 45, 843–863.
- Pistolesi, M., A. Bertagnini, A. Di Roberto, R. Isaia, A. Vona, R. Cioni and G. Giordano (2017). The Baia-Fondi di Baia eruption at Campi Flegrei: stratigraphy and dynamics of a multi-stage caldera reactivation event. *Bull. Volcanol.*, 79(9), 67.
- Revil, A., A. Finizola, T. Ricci, E. Delcher, A. Peltier, S. Barde-Cabusson, G. Avard, T. Bailly, L. Bennati, S. Byrdina, J. Colonge, F. Di Gangi, G. Douillet, M. Lupi, J. Letort and E. Tsang Hin Sun (2011). Hydrogeology of Stromboli volcano, Aeolian Islands (Italy) from the interpretation of resistivity tomograms, self-potential, soil temperature and soil CO₂ concentration measurements. *Geophys. J. Int.*, 186(3), 1078–1094.
- Rey, A., E. Pegoraro, V. Tedeschi, I. De Parri, P.G. Jarvis and R. Valentini (2002). Annual variation in soil respiration and its components in a coppice oak forest in Central Italy. *Global Change Biol.*, 8(9), 851–866.
- Rosi, M., and A. Sbrana (1987). Phlegraean Fields. *Quad. Ric. Sci.*, 175 pp.
- Rosi, M., A. Sbrana and C. Principe (1983). The Phlegraean Fields: Structural evolution, volcanic history and eruptive mechanisms. *J. Volcanol. Geotherm. Res.*, 17(1-4), 273–288.
- Scarpato, C., P. Cole and A. Perrotta (1993). The Neapolitan Yellow Tuff—a large volume multiphase eruption from Campi Flegrei, southern Italy. *Bull. Volcanol.*, 55(5), 343–356.
- Serri, G.F., F. Innocenti and P. Manetti (1993). Geochemical and petrological evidence of the subduction of delaminated Adriatic continental lithosphere in the genesis of the Neogene-Quaternary magmatism of central Italy. *Tectonophysics*, 223, 117–147.
- Selva, J., G. Orsi, M.A. Di Vito, W. Marzocchi and L. Sandri (2012). Probability hazard map for future vent opening at the Campi Flegrei caldera, Italy. *Bull. Volcanol.*, 74(2), 497–510.
- Smith, V.C., R. Isaia and N.J.G. Pearce (2011). Tephrostratigraphy and glass compositions of post-15 kyr Campi Flegrei eruptions: implications for eruption history and chronostratigraphic markers. *Quat. Sci. Rev.*, 30, 3638–3660.
- Vitale, S., and R. Isaia (2014). Fractures and faults in volcanic rocks (Campi Flegrei, southern Italy): insight into volcano-tectonic processes. *Int. J. Earth Sci.*, 103(3), 801–819.
- Wohletz, K., L. Civetta and G. Orsi (1999). Thermal evolution of the Phlegraean magmatic system. *J. Volcanol. Geotherm. Res.*, 91(2-4), 381–414.
- Wohletz, K., G. Orsi and S. de Vita (1995). Eruptive mechanisms of the Neapolitan Yellow Tuff interpreted from stratigraphic, chemical, and granulometric data. *J. Volcanol. Geotherm. Res.*, 67(4), 263–290.
- Zablocki, C.J. (1976). Mapping thermal anomalies on an active volcano by the self-potential method, Kilauea, Hawaii. *Proceedings, 2nd UN Symposium of the development and use of geothermal resources, San Francisco, May 1975*, pp. 1299–1309.
- Zlotnicki J., S. Michel and C. Annen (1994). Anomalies de polarisation spontanée et systèmes convectifs sur le volcan du Piton de la Fournaise (Ile de la Réunion, France). *C. R. Acad. Sci. Paris*, 318, 1325–1331.

CORRESPONDING AUTHOR: Luca TARCHINI,

Dipartimento Scienze, Università Roma 3

Rome, Italy

email: luca.tarchini@ingv.it

© 2019 the Istituto Nazionale di Geofisica e Vulcanologia.

All rights reserved